

A QUADRATURE LASER INTERFEROMETER FOR ACCELEROMETER CALIBRATION

Robert D. Sill, Endevco®

A quadrature Michelson laser interferometer system was designed for the absolute calibration of accelerometers and other vibration transducers in accordance with Method 3 of ISO 16063-11. In contrast to conventional fringe counting or fringe disappearance methods, which only measure displacement, this technique uses a polarized laser and two photodetectors in a manner that also provides phase information of the Unit-Under-Test (UUT) output. In addition, the frequency range is greatly extended, providing repeatable data over the range from below 1 Hz to as high as 50 kHz, even though displacements at high frequencies can be smaller than a wavelength of the helium-neon light. The technique provides accurate measurements of such displacements by performing an analysis that effectively calibrates the photodetectors in the range between fringes. Other algorithms are described which reconstruct the displacement time history and pick out the complex acceleration at the vibration frequency. Also described is an air bearing shaker designed for this system, utilizing a stiff beryllium armature for low relative motion at all frequencies in a back-to-back calibration arrangement, placing the UUT on top and the mirror underneath.

INTRODUCTION

It is recommended, when re-calibrating accelerometers for sensitivity and phase response as a function of frequency, that the resonance frequency of the transducer be included in the range of frequencies tested

Manufacturers of accelerometers recommend, when re-calibrating accelerometers for sensitivity and phase response as a function of frequency, that the resonance frequency of the transducer be included in the range of frequencies tested. This can be a challenge to calibration laboratories that try to perform a calibration with minimized measurement uncertainty in a cost-effective manner. A wider bandwidth is often associated with larger uncertainties and higher cost.

There are two classes of calibration, absolute and comparison. By definition, absolute calibrations provide direct traceability of a measurement to internationally recognized fundamental quantities. Comparison calibrations, in contrast, use a standard transducer which itself has been calibrated with traceability to absolute standards. It follows that comparison calibrations will have uncertainties larger than absolute calibrations, since every step in the chain adds to uncertainty. These secondary comparison calibrations tend also to be less expensive because the equipment and techniques are less elaborate and easily automated.

The quadrature laser interferometric technique described in this paper reduces the labor and system complexity, and is capable of expanding the frequency to as high as 50 kHz.

Absolute calibrations historically are expensive, particularly at frequencies above 1 kHz, where conventional fringe counting techniques cannot be used. Laser interferometry services provide acceleration sensitivity uncertainties as low as 0.5% (confidence level 95%), and typically cost thousands of dollars per calibration, whereas cost of comparison calibrations are an order of magnitude less, with collective uncertainties generally two to five times larger. The quadrature laser interferometric technique described in this paper reduces the labor and system complexity, and is capable of expanding the frequency to as high as 50 kHz. The result is an absolute calibration with cost comparable to that of a comparison calibration, yet which maintains the superior uncertainty of an absolute calibration.



MICHELSON INTERFEROMETER

Interferometry commonly involves splitting and recombining a beam of single-frequency coherent laser light, as shown in Figure 1.

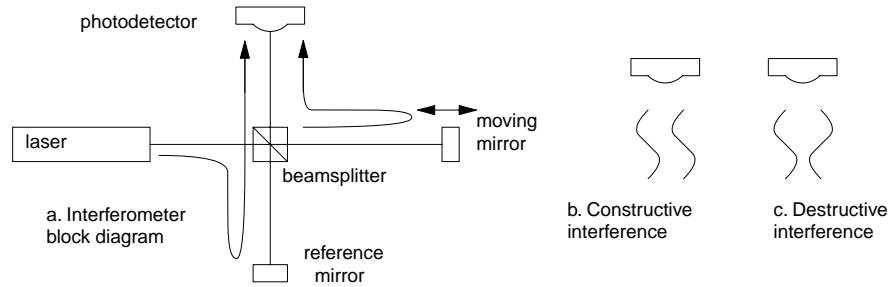


Figure 1. Michelson Interferometer.

The beam from the laser on the left in Figure 1a is split into two. One beam goes to a stationary reference mirror and so has a fixed path length. The other beam travels to a moving mirror. If the two optical path lengths are equal or differ by an integer number of wavelengths, the recombined beams will be in phase with each other and interfere constructively (Figure 1b), and maximum brightness will be sensed by the photodetector. At the opposite extreme (Figure 1c) the path lengths differ by an additional one-half wavelength, the two beams destructively interfere, and photodetector output is at a minimum.

The wavelength of red Helium-Neon laser light is an intrinsic standard, internationally accepted to be 0.63282 micrometer in air, stable to within ten parts per million for commonly encountered values of barometric pressure, humidity and laboratory temperatures [1], [2]. Since the mirror needs only to travel 1/2 wavelength to change the total path length by a wavelength, every light/dark cycle of photodetector output (called a “fringe”) represents 0.31641 +/- 0.000003 micrometers of mirror displacement.

The large number of fringes makes achievement of high-resolution measurements at low frequencies possible. For example, peak to peak displacement at 100 m/s² at 160 Hz would be 198 micrometers, or 625 fringes, giving 1250 counts per period of vibration. The total count is made over long time intervals to minimize errors [3] [4]. However, for vibration at high frequencies and reasonable amplitudes, displacements are generally too small to create a fringe. Rather than a digital count of fringes, the measurement becomes an estimate of what fraction of a fringe the motion represents. For instance, at 100 m/s² and 20 000 Hz, the peak to peak displacement of 12.7 nm would represent only 4% of one fringe. With a single detector, this determination is very difficult, since the variation of photodetector output is severely dependent on the average position in the mirror. This is shown in Figure 2.

The large number of fringes makes achievement of high-resolution measurements at low frequencies possible.

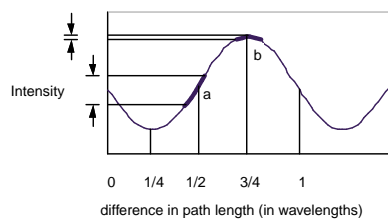


Figure 2. Intensity variation as a function of path length difference.

Best photodetector resolution occurs at position “a” in Figure 2, at which the average mirror position causes

the photodetector to be midway between the peak and valley of intensity. The slope of the curve, that is, the change of light intensity as a function of mirror position, is at a maximum. Poorest resolution occurs when the average mirror position causes intensity extremes, whether from maximal constructive or destructive interference between the beams (such as position “b”). For vibration amplitudes smaller than a wavelength (shown as thickened portion of the waveform), intensity variation (and therefore change of voltage output) around position “b” would be very small. In such an unfortunate condition, it would be useful to be able to reposition one of the mirrors to change path length by $\frac{1}{4}$ wavelength, so that the photodetector would have maximum sensitivity, as in “a”. The quadrature laser effectively solves the problem by using two interferometers, one of which has a path length $\frac{1}{4}$ wavelength longer than the other, so one is always near the point of maximal resolution.

THE QUADRATURE LASER INTERFEROMETER

The quadrature interferometer uses a polarized laser, two photodetectors and an optical trick. The laser is oriented so the polarization axis is rotated 45 degrees with respect to the alignment of the beam splitters and reference mirror (see Figure 3). The one polarized beam oriented at this angle is vectorially equivalent to two beams of equal intensity occupying the same space, designated V and H, one polarized vertically and one horizontally. The two beams are ultimately separated with a polarizing beam splitter, and using a photodetector for each beam, two interferometers are created from these components.

The quadrature interferometer uses a polarized laser, two photodetectors and an optical trick.

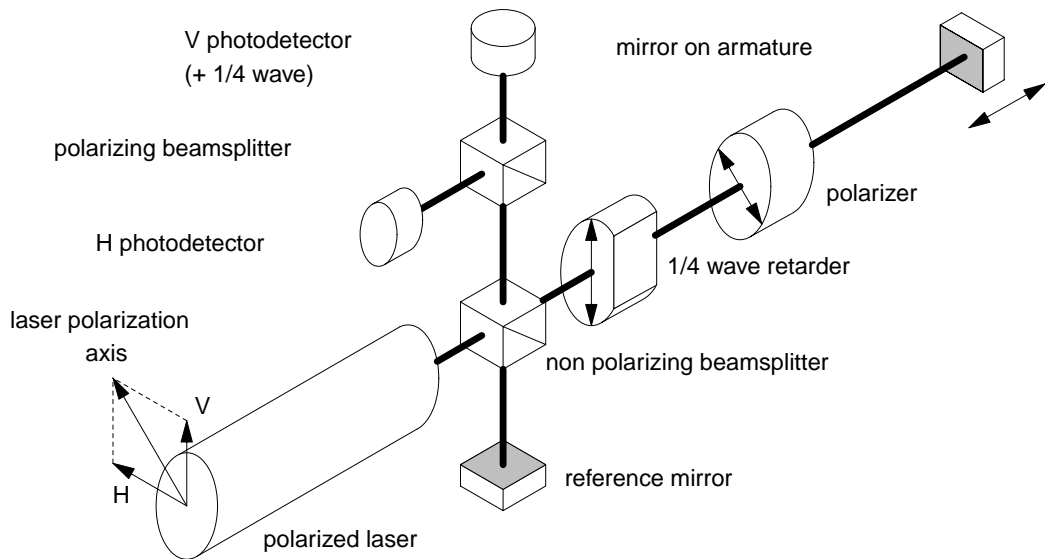


Figure 3. Exploded view of a quadrature laser interferometer. *This is one of many possible implementations. Other designs, and theory on quadrature interferometers for use at high frequencies, are given in reference [5].*

A polarized device called a $\frac{1}{4}$ wave retarder, is designed to slow light polarized in its axis more than the light polarized perpendicular to its axis.

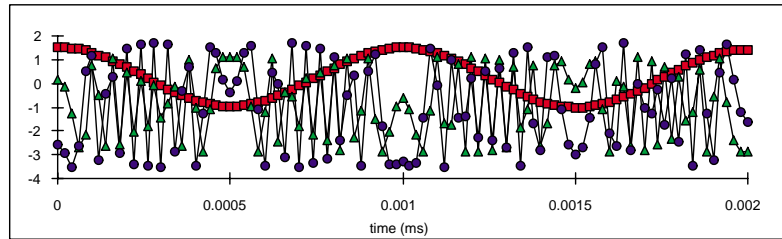
The trick is provided by a polarized device called a $\frac{1}{4}$ wave retarder, which is designed to slow light polarized in its axis more than the light polarized perpendicular to its axis. Its axis is placed in parallel with the polarization of beam “V”, effectively adding $\frac{1}{4}$ wavelength to its path. That photodetector output will always differ by $\frac{1}{4}$ of a fringe, or 90 degrees, from the other. (The term to describe this relationship between the two outputs is that they are *in quadrature*, which explains the name given to the laser.) Referring back to Figure 2, no matter where the mirror is, one or both of the photodetectors will have high sensitivity.

Actually the $\frac{1}{4}$ wave retarder does its trick twice, once as the beam travels to the armature mirror and again on the way back. The effect of the first time through is ignored, that is, undone by the polarizer, which is positioned so that polarization of the beam returning from the mirror has been restored to the same polarization as the laser before it passes through the retarder the second time.

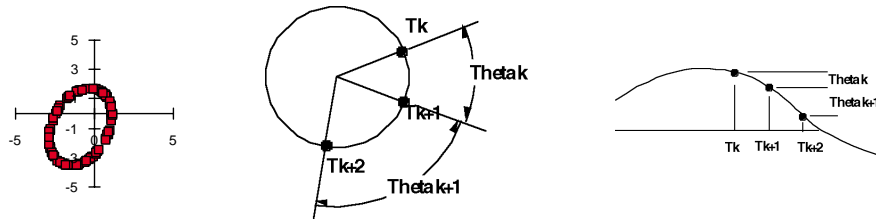
THE ALGORITHMS: RECONSTRUCTING DISPLACEMENT

This high sensitivity, coupled with the algorithms described below, allows the quadrature laser to be used for measurements of displacements much smaller than a wavelength of light.

This high sensitivity, coupled with the algorithms described below, allows the quadrature laser to be used for measurements of displacements much smaller than a wavelength of light. In addition, the relationship between the two photodetectors outputs allows determination of the direction of the displacement. This technique is illustrated in Figure 4. As will then be described, this means UUT phase can be measured.



a. Simulated voltage outputs from photodetectors H and V (circles and triangles) superimposed on sinusoidal 1 kHz vibration (squares), all plotted as a function of time.



b. Photodetectors (H vs. V) c. Determining angle d. Reconstruction of displacement

Figure 4. Determination of displacement from quadrature signals. *The relationships between photodetector and vibration waveforms are visible in a. For example, the decrease in fringe rate and reversal of phase are seen when vibration stroke nears its endpoints. It may be easier to visualize this vibration direction using the Lissajous pattern in b, in which the sequence of plotted data pairs can be imagined to fall in the elliptical pattern in either a clockwise or counterclockwise manner. An algorithm performs this analysis in several steps, first with a transformation of data pairs from an elliptical to a circular path. As shown in c, each data pair at time T_k represents an angular position given by $\arctan(V_k/H_k)$. Differences between angles for each time step k , for example Θ_k , are summed over time, to give the reconstructed total angle as a function of time, shown in d. Total angle directly represents displacement, since each 360 degrees of fringe angle represents another 0.31641 micrometer.*

Further description is needed of the intermediate steps of the algorithm. An important step is the transformation of photodetector data. The orbit defined by the Lissajous pattern will not be perfectly circular for several reasons. Misalignment of the beams will reduce the amount of light captured by one or both detectors; offsets and gains of the photodetector circuitry are not ideal; and the polarization angle between the two beams is not necessarily 90 degrees. All of these factors will cause the orbit to be elliptical in shape. Uncorrected, this can cause significant errors if trying to estimate displacements of only a fraction of a wavelength. The solution is an algorithm using a least squares fit [6] that determines coefficients that can be applied to the photodetector data to transform the ellipse to a circle. With the transformation, the system effectively calibrates

and compensates for deviations from ideal photodetector output. The transformed pairs of photodetector data points represent easily calculated angular positions of the cycle. Summing differences between pairs through the data set, the displacement history is constructed, as was shown in Figure 4d.

The reconstructed waveform is then analyzed with the Convolution Technique described below to determine peak sinusoidal displacement amplitude and phase (which in the initial step is calculated with respect to the common trigger time of the data acquisition of the laser and UUT channels) at the vibration frequency. Then the peak displacement value is multiplied by the square of $2\pi f$ to get peak acceleration. By taking the ratio of the UUT output (also analyzed with the Convolution Technique) to the acceleration, sensitivity is determined. Phase of the UUT is then calculated as the difference between the phase of the UUT waveform and that of the reconstructed laser displacement waveform. (The need for simultaneous triggering of all data acquisition channels, to accurately determine phase, is apparent.)

THE ALGORITHMS: CONVOLUTION TECHNIQUE

Superimposed lower frequency motions are used to guarantee that the photodetectors see a complete peak to valley cycle.

At high frequencies the overall motion might be so small the photodetector pairs do not trace an entire orbit from which to define the transformation. Superimposed lower frequency motions are used to guarantee that the photodetectors see a complete peak to valley cycle. For example, it is useful to apply a small step to the power amplifier input to offset the armature position, so the armature drifts back to its equilibrium position while the high frequency vibration occurs. The reconstructed displacement shows this drift as a displacement slope superimposed on the vibration. Because this drift represents a superposition of frequencies at other than the fundamental vibration frequency, it is necessary to use a narrow band-pass filter in the algorithm to pick out the amplitude of only the desired vibration frequency.

Such techniques are referred to in ISO 16063-11, the international standard for laser calibration, which describes three methods of interferometry. The first two are those historically used: the “Fringe counting method” and the “Minimum point method”. The third method describes the use of quadrature lasers, as in this paper. The Standard calls this the “Sine-approximation method”, and describes a least squares fit of the constructed displacement history to a theoretical sinusoid of the same frequency. Allowance is given for the use of other algorithms, such as the Convolution Technique described below, provided they meet the uncertainty requirements of <0.5% uncertainty at reference conditions, and <1% to 10 kHz. (It is the aim of this paper is to show that the algorithms exceed these requirements, and that this laser implementation conforms to the standard.)

The Least Squares Sine Approximation technique is effective when applied to a small number of cycles of the vibration frequency (such as would be likely at low vibration frequencies). In most conditions the Convolution Technique is more effective at rejecting noise and harmonic distortion, particularly when many cycles of data are available to analyze, such as at higher frequencies. Figure 5 shows the comparison of the harmonic rejection efficiency of the Convolution Technique described below to the Least Squares Sine Approximation.

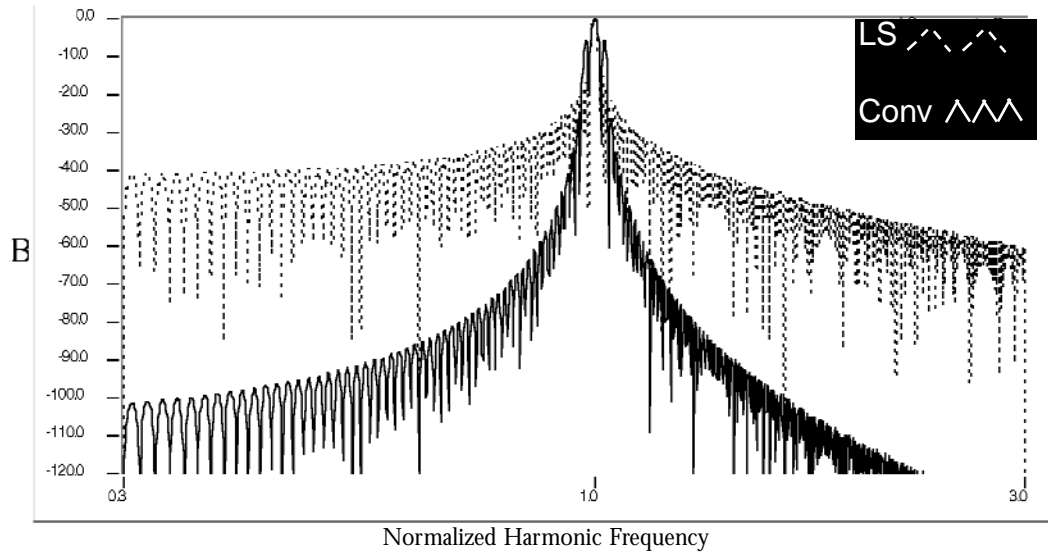


Figure 5. Comparison of Least Squares Sine Approximation to Convolution Technique.
 The horizontal axis is frequency ratio of distortion to the fundamental, and the vertical axis is the rejection of the distortion using a sample window with exactly 40 cycles of the fundamental period, plotted logarithmically in dB. Note the Convolution Technique distortion rejection is better at all frequencies except two closely spaced lobes on either side of the fundamental.

At each frequency, a digital snapshot of the reference and UUT waveforms are taken.

The Convolution Technique emulates a frequency response analyzer. At each frequency, a digital snapshot of the reference and UUT waveforms are taken, with the sample length carefully chosen so the number of cycles is an integer multiple of the fundamental frequency's period. (Listed in Table I, 80 cycles was chosen for typical reference conditions of 100 or 160 Hz, so that an integer number of both power line cycles and the typical reference frequency are included, to maximize power line frequency rejection.) The waveforms are then multiplied, point-by-point, by a haversine weighting function the same length as the sample, as shown in Figure 6.

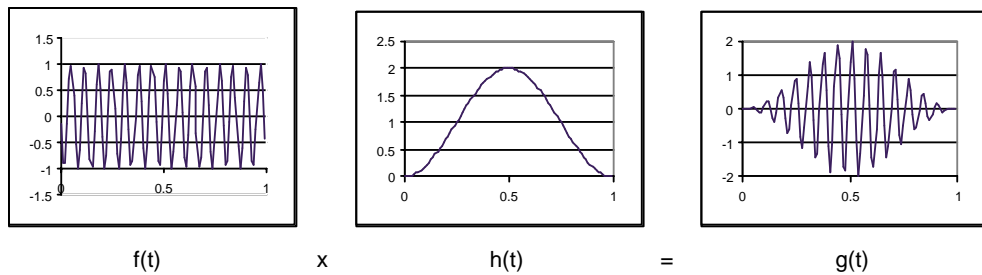


Figure 6. First step of the Convolution Technique.
 The original waveform $f(t)$ is multiplied by a haversine of a length equal to an integer number of cycles of the fundamental frequency.

The waveforms from that operation then go through a convolution process: each is then multiplied point-by-point by the theoretical value of a cosine of the fundamental vibration frequency and summed; the same operation is performed with a sine, shown in Equations 1-4.

$$(1/N) \times \Sigma(g(t) \times \cos(2\pi ft)) = \mathbf{Re} \quad (1)$$

$$(1/N) \times \Sigma(g(t) \times \sin(2\pi ft)) = \mathbf{Im} \quad (2)$$

$$\mathbf{Ampl} = \sqrt{(\mathbf{Re}^2 + \mathbf{Im}^2)} \quad (3)$$

$$\mathbf{Phase} = \tan^{-1}(\mathbf{Im}/\mathbf{Re}) \quad (4)$$

As in a quadrature demodulator, the sums resulting from the multiplication with a cosine and sine represent the real and imaginary components of the waveforms, respectively, with respect to the input. Amplitude of the fundamental component is then the root-sum-square of the two complex components **Re** and **Im**. Phase is the arctangent of the ratio **Im/Re**.

The efficiency of the technique for rejecting noise and harmonics is a strong function of the number of cycles of the fundamental frequency.

The efficiency of the technique for rejecting noise and harmonics is a strong function of the number of cycles of the fundamental frequency. This is illustrated in Figure 7. When only one period of the vibration is captured, the least squares technique is superior to the Convolution Technique in rejection of extraneous noise.

Freq (Hz)	Pk-Pk disp (m)	Fringes (He-Ne)	Accel (g)	Fringe Freq (Hz)	Velocity (m/s)	Sample Rate (Hz)	Cycles	Number of Samples
1	1.0E-02	31604.81	0.02	99289	0.0314	500000	4	200000
2	1.0E-02	31604.81	0.08	198579	0.0628	500000	8	200000
5	1.0E-02	31604.81	0.50	496447	0.1571	2000000	5	200000
10	1.0E-02	31604.81	2.01	992894	0.3142	5000000	4	200000
20	1.0E-02	31604.81	8.05	1985789	0.6283	5000000	8	200000
50	2.0E-03	6280.64	10	986561	0.3122	5000000	20	200000
100	5.0E-04	1570.16	10	493281	0.1561	2000000	80	160000
200	1.2E-04	392.54	10	246640	0.0780	1000000	80	40000
500	2.0E-05	62.81	10	98656	0.0312	500000	80	8000
1000	5.0E-06	15.70	10	49328	0.0156	200000	80	16000
2000	1.2E-06	3.93	10	24664	0.0078	200000	80	8000
5000	2.0E-07	0.63	10	9866	0.0031	500000	80	8000
10000	5.0E-08	0.16	10	4933	0.0016	1000000	80	8000
20000	1.2E-08	0.04	10	2466	0.0008	2000000	80	8000
50000	2.0E-09	0.01	10	987	0.0003	5000000	80	8000

Table I. Parameters for Calibration by Laser Interferometry. *The values listed are representative of practical limits of the system. Acceleration is limited at low frequencies to 10 mm displacement for the shaker or 10 g, whichever is smaller. At frequencies with high velocities, the sample rate required to capture the fringe frequency without aliasing consumes large amounts of memory, so the total capture time is limited by the buffer size.*

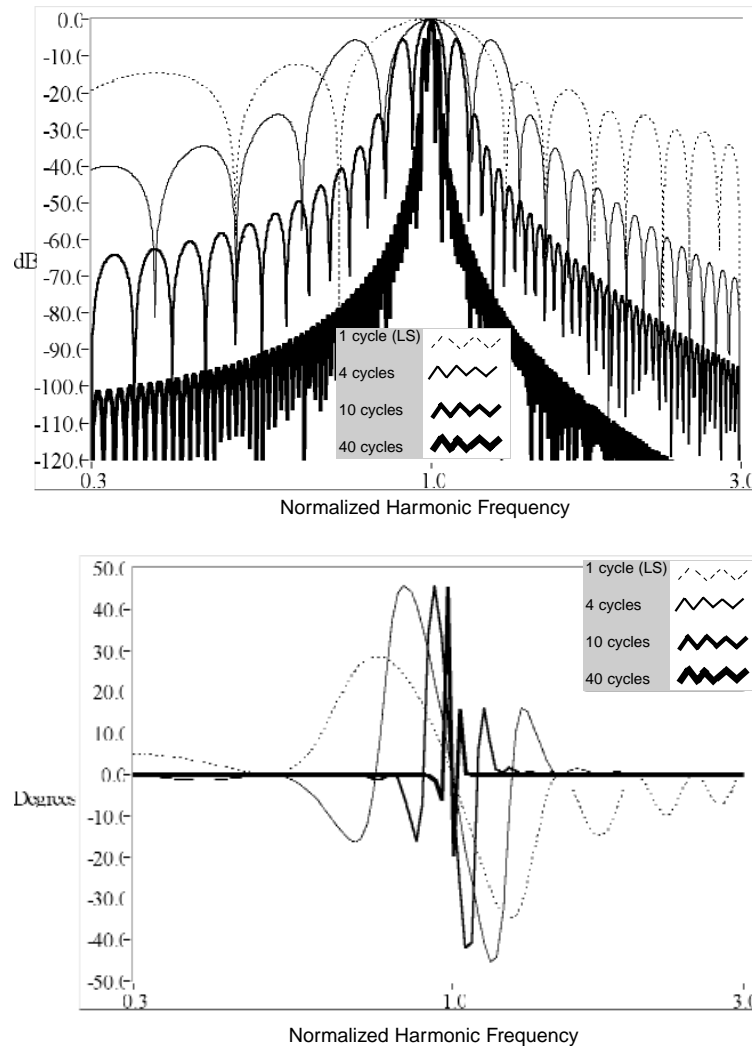


Figure 7. Harmonic rejection efficiency of Convolution Technique. The horizontal axis is harmonic frequency normalized by the fundamental vibration frequency. The vertical axis of the upper graph is the amplitude rejection ratio, in decibels, of the harmonic superimposed on the fundamental frequency. Vertical axis on the lower graph is the phase error in degrees if the amplitude of the noise component was as large as the amplitude of the fundamental vibration frequency. Errors in both amplitude and phase would scale with the relative size of the noise (for example, harmonics of approximately 10% of the signal amplitude close to the fundamental frequency would cause about 4 degrees error). Each of the four curves represents the effect of the sample rate, where “cycles” are the integer number of periods of the vibration frequency in the analyzed sample. In the case the entire sample consists of only one period, a Least Squares fit is used rather than the Convolution Technique (designated “LS”).

The acceleration is calculated by multiplying displacement amplitude by the square of $2\pi f$. The amplitude of the output of the UUT is determined with the same Convolution technique. The next step is taking the ratio of the UUT amplitude to the laser-determined acceleration and correcting for any known gain and phase deviations of the signal conditioning paths to get the UUT sensitivity. Mass loading errors, if any, are corrected according to reference [7].

THE SHAKER/ISOLATION ASSEMBLY

In conjunction with the laser, a new shaker and isolation system was developed to allow back-to-back calibration. As shown in Figure 8, the laser is located beneath the shaker, shining up through the magnet to the mirror on the underside of the armature, with the UUT mounted conventionally on top. The armature is made of solid beryllium, giving exceptionally low relative motion between the mirror and the top surface. (Since the stiffness of beryllium is 40% higher than steel, yet density is 2/3 that of aluminum, the longitudinal resonance frequency between the mirror and a 15 gram UUT is on the order of 200 kHz. This would imply a mass loading effect of only 1% at 20 kHz and 0.5 dB at 50 kHz, to a large degree correctable per reference [7].)

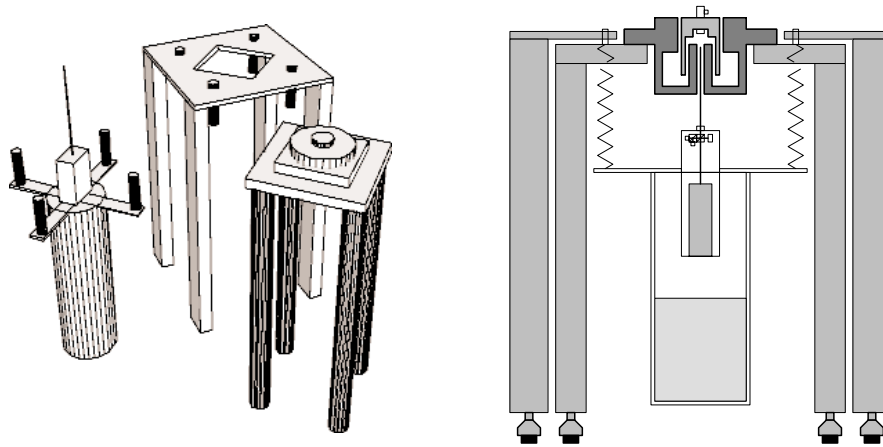


Figure 8. Shaker, laser and isolation assembly. *The laser is shown in its isolation mount with its beam directed upward to the mirror. Lead shot in the laser ballast keeps the center of gravity low for pointing stability. The isolation assembly hangs from four springs from the Laser Table (the springs are shown split in the exploded view, with half on the ballast and half under the Laser Table connected to adjustment screws). The shaker on its table pokes up through the diagonal hole in the Laser Table. The laser isolation nestles between the Shaker Table legs. The only contact between the two tables is through the floor, and every leg has a rubber isolation foot.*

The stroke of the armature is greater than 1 cm, and alignment of the laser beam during vibration is maintained with a narrow gap air bearing. The bearing has ceramic-coated surfaces on both internal and outer diameters, and two circumferential rows of orifices with 1.27 cm vertical separation to provide resistance to rocking. The orifices have resistance to flow comparable to the fluid resistance in the gap, to provide self-centering characteristics. (There is an appreciable pressure drop from the orifice to the top or bottom of the armature, giving net radial forces that normally cancel. If there is a transverse load pushing the armature against one sidewall, the gap locally decreases and resistance to flow increases. On the diametrically opposite side, the gap increases and radial pressure drops. Net force pushes the armature back to the center.)

It is necessary to isolate the laser from forces, whether from the environment or from the shaker.

It is necessary to isolate the laser from forces, whether from the environment or from the shaker. An accelerometer is an inertial device, measuring absolute acceleration. The interferometer measures changes in the relative path length between it and the armature, so to measure absolute motion it must not move. This is an impossible requirement. Fortunately, reviewing the efficiency of the Convolution Technique, the requirement is relaxed so that the isolation system needs to minimize transmission of forces at the vibration frequency.

Isolation from the environment is solved with a compliant mount of a massive system. The resonance of the mount was approximately 1.1 Hz, using approximately 20 cm of static deflection of extension springs. Cables to the shaker and laser must be strain isolated to prevent transmission of forces between the two tables.

RESULTS AND CONCLUSIONS

The system is easily set up, aligned and used.

The system is easily set up, aligned and used. Physical and electrical stability is good: alignment is maintained over periods of months, and repeatability of measurements is better than 0.1%. The robustness of the system is being proven with continuing tests at Endeveco. A thorough report of capabilities will be published in the near future. Results so far are in good agreement with NIST (see an example in Figure 9).

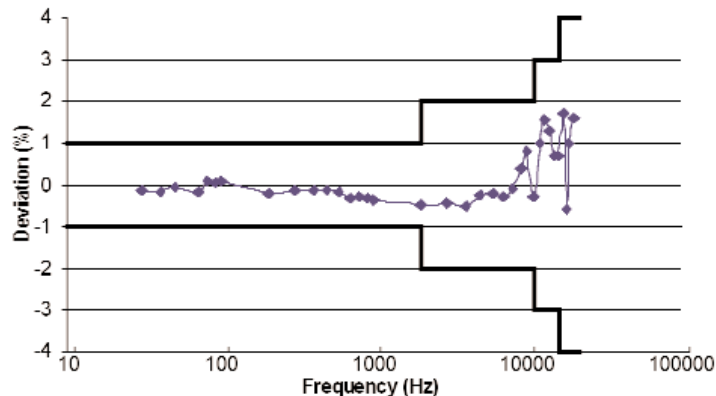


Figure 9. Results from NIST and the quadrature laser. Plotted are the calculated differences between results of tests at NIST and on the Endeveco's quadrature laser on an Endeveco Model 2270M8 s/n AL879. The thickened lines are the stated 2 sigma uncertainties by NIST.

Vibration isolation is successful across nearly the entire 2 Hz to 50 kHz range. A few narrow-band frequency regions require additional attention to achieve nearly continuous sweeps, as opposed to the rather sparse third-octave frequency spacing of international standards. These widely spaced frequencies are adequately covered by the system as it is now.

The control software has algorithms to monitor the parameters that affect the measurement, such as the quality of the laser output, distortion in vibration and transducer waveforms, standard deviations of sensitivities. The software screen in a test from 5 Hz to 50 kHz is shown in Figure 10.

ENDEVCO TP 316

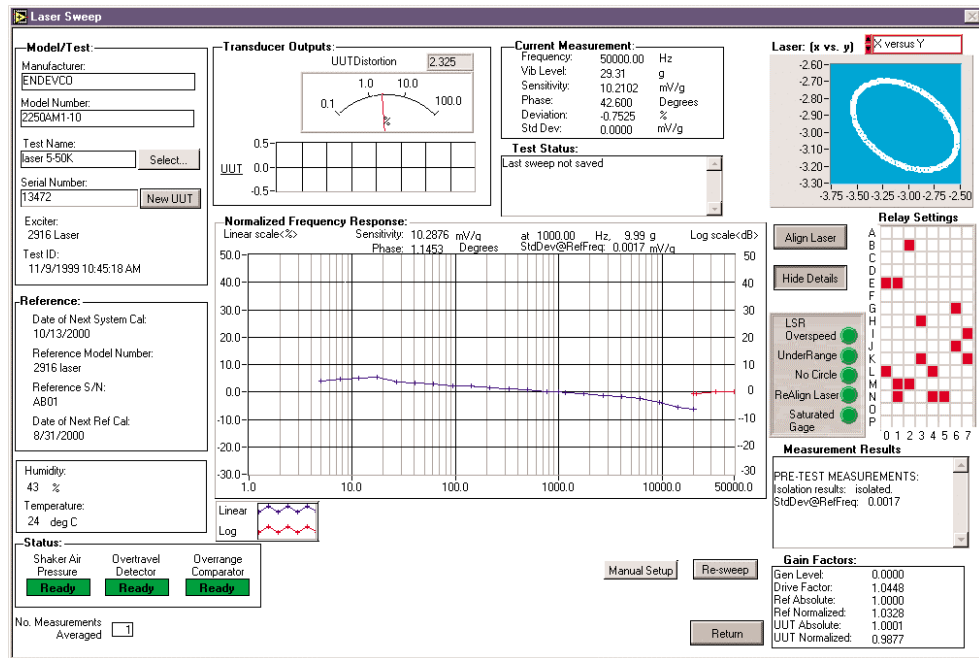


Figure 10. Software output of Automated Accelerometer Calibration System with the quadrature laser. Visible are the measurement results of sensitivity, frequency response, distortion, and environmental parameters. The Lissajous pattern of the photodetectors and the many status indicators are seen on the right.

The quadrature laser, unique algorithms, improved shaker and novel isolation design make a practical absolute calibration system which is available as an addition to the Endevco Automated Accelerometer Calibration System. The system meets or exceeds the capabilities described in the new international standard.



BIOGRAPHY

ROBERT D. SILL received his Bachelor of Science and Master of Engineering degrees in 1977 from Harvey Mudd College and joined Endevco in 1978.

He is a Senior Scientist in the Silicon Engineering group, specializing in silicon microsensors, shock transducers and calibration equipment.

REFERENCES

- [1] German and Corcoran, "Measuring the Variable Speed of Light Improves Laser Distance Measurement", Electronics, Apr 24, 1972.
- [2] ISO 16063-11, Methods for the calibration of vibration and shock transducers – Part 11: Primary vibration calibration by laser interferometry.
- [3] Hans-Jurgen von Martens, "Interferometric Counting Methods for Measuring Displacements in the Range of 10^{-9} m to 1 m", Metrologia, 24, 163-170 (1987).
- [4] Hans-Jurgen von Martens, "On the Errors and Uncertainties of Interferometric Measurements of Linear and Torsional Vibrations", SPIE, Vol. 2358, Vibration Measurements (1994).
- [5] Scruby, C. B. and Drain, L. E., Laser Ultrasonics: Techniques and Applications, Adam Hilger, New York, pg 119.
- [6] Heydemann, Peter L. M., "Determination and correction of quadrature fringe measurement errors in interferometers". Applied Optics, 20, No 19, pp. 3382-3384, 1981.
- [7] Robert D. Sill, "Mass Loading in Back-to-Back Reference Accelerometers", Technical Paper 310, Endevco Corporation.

ACKNOWLEDGMENTS

The author wishes to thank and acknowledge the work of Alexander (Sasha) Morzhakov, Iouri (Yuri) Kudrioshov, and Sergey Svezhintsev of VolgATec, Ltd, Russia, Lewis C. Ensor, retired from Endevco Corporation, and Sandra Arabe Smith of Endevco Corporation.